Toroidal drift precession and wave - particle interaction in shaped tokamaks with finite beta and neoclassical equilibrium effects

Jonathan P. Graves[1]
[1]École Polytechnique Fédérale de Lausanne (EPFL), Centre de Recherches en Physique des Plasmas, Association EURATOM-Confédération Suisse, 1015 Lausanne, Switzerland
(Dated: May 10, 2019)

The drift kinetic equation is analysed for linear instabilities that are sensitive to the toroidal drift motion of long-mean free path particle populations. The interaction Lagrangian is resolved, and the toroidal drift precession evaluated for realistic tokamak equilibria, including the effects of cross section shaping and finite beta. The drift kinetic equation is expanded around a flux surface in accordance with a neoclassically resolved equilibrium and coincident bootstrap current. Analytical results pertaining to the effect of shaping, magnetic shear and finite beta on the toroidal drift and bounce/transit frequencies of passing and trapped particles are shown.

PACS numbers:

I. INTRODUCTION

Instabilities sensitive the drift motion of particles with long mean free path are in turn sensitive to the geometry of the magnetic equilibrium. Collisionless wave-particle interaction can be driven by the resonance between the wave frequency, the toroidal drift precession and/or the bounce or transit frequency. Moreover, the Lagrangian of the system is also related to the drift motion of the particles. Papers by e.g. Rosenbuth and Sloan [1], Connor *et al* [2] and Jucker *et al* [3] clearly demonstrate the sensitive effect of the magnetic equilibrium on the drift precession depends, since it is seen that if the ballooning parameter $\alpha = -q^2 d\beta/d\epsilon$ (with q the safety factor, $\beta = 2P/B^2$ the ratio of thermal and magnetic energy, $\epsilon = r/R_0$ the ratio of the local minor radius and the major radius) is of order unity, the effect of pressure gradient modifies the toroidal drift of trapped particles at leading order (in the case of Ref. [3] anisotropic pressure was assumed).

The drift motion of circulating particles is important close to a rational surface where the parallel wave-number is small. While the drift motion of deeply circulating (small magnetic moment $\mu = v_\perp^2/(2B)$) is formally an order of epsilon smaller than for trapped particles, the effect of pressure, which manifests itself primarily through the Shafranov shifted equilibrium, is strong [4]. Indeed, for $\alpha \sim 1$ the toroidal drift for passing particles is the same order as that of the trapped particles. Since the Lagrangian of the system is related to the toroidal drift precession, this implies that in principle passing particles can efficiently drive instability (in practice one also requires, amongst other factors, that the parallel wave number is also small, which occurs where q is nearly rational). There is clearly a need to investigate the physical dependencies of the toroidal drift of circulating particles for all pitch angles, especially close to the passing-trapped boundary. In particular, it has recently been seen [5, 6] that barely trapped and possibly barely passing particles can interact with MHD oscillations called the electron fishbone instability. For this application, it might be of interest to investigate the effect of plasma cross section shaping, since electron fishbones are notably observed in circular machines operating with radially extended low shear (where $q \approx 1$) q-profiles (although electron fishbones have been observed in DIII-D [6] where additional NBI heating was employed). Indeed the TCV tokamak is usually used with conventional (elongation $\kappa \approx 1.4$ and triangularity $\delta = 0.3$) or strong shaping, and despite the tokamak being equipped with steerable electron cyclotron heating (ECH) with record power density, electron fishbones have not yet been identified. Nevertheless, it is known that plasma shaping in TCV has an impact on Trapped Electron Modes (TEMs) [7], and in particular, the effect of triangularity on TEMs has in part been attributed to the modification of the toroidal drift of trapped particles.

The magnetic shear has a very strong effect on the toroidal drift precession. This is particularly true for passing particles. In order to investigate the impact of toroidal drift motion in the perturbed drift kinetic equation it is necessary to first establish precisely the distribution of the passing particles in the equilibrium. The differing expressions for the shear dependent terms in [5] and [8] can impact very strongly on the fishbone resonance condition, and consequently it is necessary to establish a valid expression, which, as seen in this paper, requires a neoclassical treatment. As a final point, there are many fast ion instabilities that are sensitive to the toroidal drift, and the parallel wave vector. It is again first necessary to examine the fast ion equilibrium distribution function including the effect of collisions and resulting bootstrap current [9]. This treatment is particularly appropriate because the neoclassical corrections to the fast ion equilibrium distribution coincide with those of an electron distribution at the appropriate limit in the tail temperature.

This paper provides a convenient expression for the perturbed drift kinetic equation, and derives a general expression for the perturbed Lagrangian in terms of the toroidal and radial drift motion. This expression is shown to be particularly powerful and convenient for fully electromagnetic MHD perturbations. The perturbed drift kinetic equation is expanded about an equilibrium distribution function that is consistent with neoclassical theory (e.g. a distribution that produces bootstrap current). Following this, the toroidal drift, bounce and transit frequencies are derived analytically in terms of Shafranov shift, shaping and aspect ratio to high order in accuracy. It is also of interest to examine the Lagrangian since this measures the energy of the instability drive. The effects of shaping, pressure and magnetic shear are investigated for all pitch angles, and new expressions are derived for deeply trapped, barely trapped/barely passing, and deeply passing. These results naturally lend themselves to some explanations for tokamak observations of TEMs, electron fishbones and other instabilities.

II. PERTURBED DRIFT KINETIC EQUATION

In this section global modes are considered, and the effects of finite radial drift excursion is retained. Following [10] the perturbed distribution function δf can be written in terms of the equilibrium distribution function $F = F(\mathcal{K}, \mu, P_\phi)$:

$$\delta f = \frac{Ze}{m} R^2 (\boldsymbol{\delta A} \cdot \boldsymbol{\nabla}\phi) \frac{\partial F}{\partial P_\phi} + \frac{Ze}{m}\delta\phi \frac{\partial F}{\partial \mathcal{K}} - \mu \frac{\delta B_\parallel}{B}\frac{\partial F}{\partial \mu} + \delta g \tag{1}$$

where the drift kinetic equation describes the kinetic contribution δg via

$$\frac{d}{dt}\delta g = -\frac{i}{m}\frac{\partial F_0}{\partial \mathcal{K}}(\omega - n\omega_*)\delta L, \tag{2}$$

and $\omega_* = (\partial F/\partial P_\phi)/(\partial F/\partial \mathcal{K})$. The perturbed Lagrangian is written

$$\delta L = Ze\boldsymbol{v}_d \cdot \boldsymbol{\delta A} - Ze\delta\phi - m\mu\delta B_\parallel,$$

with equilibrium drift velocity

$$\boldsymbol{v}_d = \frac{\boldsymbol{B}}{B} \times \left\{ \frac{\boldsymbol{\nabla}\Phi}{B} + \frac{1}{\Omega_c}\left(\mu\boldsymbol{\nabla}B + v_\parallel^2 \boldsymbol{\kappa}\right)\right\},$$

where m is the particle mass, Ze is the particle charge, $\Omega_c = eZB/m$, the equilibrium electric field is $\boldsymbol{E} = -\boldsymbol{\nabla}\Phi$, and $\boldsymbol{\kappa} = (\boldsymbol{B}/B)\cdot\boldsymbol{\nabla}(\boldsymbol{B}/B)$. Here the constants of motion are $P_\phi = (Ze/m)\psi + Rv_\parallel \boldsymbol{B}\cdot\boldsymbol{\nabla}\phi/(B|\boldsymbol{\nabla}\phi|)$ the toroidal canonical momentum (R is the major radius), $\mathcal{K} = \mathcal{E} + Ze\Phi/m$, $\mathcal{E} = v^2/2$ and $\mu = v_\perp^2/(2B)$, where ψ is the poloidal flux which is related to the local minor radius with $d\psi/dr = rF(r)/qR_0$. Here $F(r)$ is related to the toroidal field, since the equilibrium magnetic field can be written

$$\boldsymbol{B} = F(\psi)\boldsymbol{\nabla}\phi + \boldsymbol{\nabla}\psi \times \boldsymbol{\nabla}\phi. \tag{3}$$

The perturbed Lagrangian can be written in a convenient form by assuming the gauge $\boldsymbol{\delta A}\cdot\boldsymbol{B} = 0$. Thus writing the magnetic vector potential $\boldsymbol{\delta A} = \boldsymbol{\xi}\times\boldsymbol{B}$ in terms of the general displacement $\boldsymbol{\xi}$ and using the Clebsch form of the vector field

$$\boldsymbol{B} = \boldsymbol{\nabla}\psi \times (\boldsymbol{\nabla}\phi - q\boldsymbol{\nabla}\theta)$$

yields the vector potential

$$\boldsymbol{\delta A} = -(\boldsymbol{\nabla}\phi - q\boldsymbol{\nabla}\theta)(\boldsymbol{\xi}\cdot\boldsymbol{\nabla}\psi) - \boldsymbol{\nabla}\psi(q\boldsymbol{\xi}\cdot\boldsymbol{\nabla}\theta - \boldsymbol{\xi}\cdot\boldsymbol{\nabla}\phi).$$

Here, and in the following expansion of the drift kinetic equation a straight field line coordinate system is employed with Jacobian $J_{\psi,\theta} = |\boldsymbol{\nabla}\psi\times\boldsymbol{\nabla}\theta\cdot\boldsymbol{\nabla}\phi|^{-1} = qR^2/F$. Following at this point Ref. [11] by defining a displacement in the form:

$$\boldsymbol{\xi} = \boldsymbol{\xi}_p + \eta\boldsymbol{B}$$

with the properties,

$$\xi^\psi = \boldsymbol{\xi}_p\cdot\boldsymbol{\nabla}\psi \;\;,\;\; \xi^\theta = \boldsymbol{\xi}_p\cdot\boldsymbol{\nabla}\theta \;\text{ and }\; \boldsymbol{\xi}_p\cdot\boldsymbol{\nabla}\phi = 0$$

leads to the following compact exact definition for the perturbed Lagrangian

$$\delta L = Ze(\xi^\psi \omega_{d0}^\phi + q\xi^\theta\omega_d^\psi) \tag{4}$$

with

$$\omega_{d0}^\phi = -(\boldsymbol{\nabla}\phi - q\boldsymbol{\nabla}\theta)\cdot\boldsymbol{v}_d - \frac{\delta\phi}{\xi^\psi} - \frac{m\mu}{Ze}\frac{\delta B_\parallel}{\xi^\psi} \tag{5}$$

and

$$\omega_d^\psi = -\boldsymbol{v}_d\cdot\boldsymbol{\nabla}\psi.$$

It will be seen that for magnetohydrodynamic (MHD) perturbations, the expression ω_{d0}^ϕ in Eq. (5) is identical to the toroidal magnetic drift in the absence of equilibrium electric field, the absence of the direct effect of magnetic shear, and the absence of the diamagnetic effect [1] on the toroidal field.

A. The toroidal magnetic drift

The full time derivative on the left hand side of the drift kinetic equation of Eq. (2) can be written as

$$\frac{d}{dt} = \left\{ v_\parallel \frac{\partial}{\partial l} + \boldsymbol{v}_d\cdot\boldsymbol{\nabla} - i\omega \right\}$$

where $\partial/\partial l = (\boldsymbol{B}/B)\cdot\boldsymbol{\nabla}$ and it has been assumed here and in Eq. (2) that perturbations are of the form $\sim \exp(-i\omega t - in\phi)$. It is further imposed that

$$\delta g = \sum_m \delta g^{(m)}(\tilde{\psi}, \theta)\exp(im\theta)$$

where

$$\tilde{\psi} = \frac{m}{Ze}P_\phi$$

is a constant of the equilibrium motion. In particular, the equilibrium distribution function F satisfies a correction about the flux label ψ such that

$$F(\hat{\psi},\mathcal{K},\mu) \equiv F(\psi,\theta,\mathcal{K},\mu) \approx F_0(\psi,\mathcal{K},\mu) + (\hat{\psi}-\psi)\frac{\partial F_0}{\partial \psi} \tag{6}$$

where

$$\hat{\psi} = \tilde{\psi} - \psi_0 = \frac{Fv_\parallel}{\Omega_c} - \psi_0 + \psi$$

and the single particle is known to follow

$$\psi = \tilde{\psi} - \frac{Fv_\parallel}{\Omega_c}. \tag{7}$$

The objective in the next section will therefore be to solve for the constant of motion ψ_0, which in turn should be consistent with neoclassical theory, and in particular it should be consistent with bootstrap current.

Continuing with examination of the full time derivative, it is useful to define

$$\dot{\theta} = \dot{\theta}_0 + \dot{\theta}_d$$

where

$$\dot{\theta}_0 = \frac{Fv_\parallel}{qBR^2} \quad \text{and} \quad \dot{\theta}_d = \boldsymbol{v}_d\cdot\boldsymbol{\nabla}\theta = -\omega_d^\theta,$$

so that

$$\frac{d\delta g}{dt} = \sum_m \exp(im\theta) \left\{ \dot{\theta}\left.\frac{\partial \delta g^{(m)}}{\partial\theta}\right|_\psi - \dot{\theta}_0 in\Delta q(\psi)\delta g^{(m)} -i(\omega + n\boldsymbol{v}_d\cdot\boldsymbol{\nabla}\phi - m\boldsymbol{v}_d\cdot\boldsymbol{\nabla}\theta)\delta g^{(m)} - \omega_d^\psi \left.\frac{\partial\delta g^{(m)}}{\partial\psi}\right|_\theta \right\} \tag{8}$$

where $\Delta q(\psi) = q(\psi) - m/n$.

Noting that

$$\left.\frac{\partial g}{\partial\theta}\right|_\psi = \left.\frac{\partial g}{\partial\theta}\right|_{\tilde{\psi}} + \left.\frac{\partial\tilde{\psi}}{\partial\theta}\right|_\psi \left.\frac{\partial g}{\partial\tilde{\psi}}\right|_\theta = \left.\frac{\partial g}{\partial\theta}\right|_{\tilde{\psi}} + \frac{\omega_d^\psi}{\dot{\theta}_0}\left.\frac{\partial g}{\partial\tilde{\psi}}\right|_\theta,$$

and expanding $\Delta q(\psi) \approx \Delta q(\tilde{\psi})[1+(\psi-\tilde{\psi})dq/d\psi]$ around the fast particle equilibrium variable $\tilde{\psi}$ gives finally,

$$\frac{d\delta g}{dt} = \sum_m \exp(im\theta) \left\{ \dot{\theta}\left[\left.\frac{\partial\delta g^{(m)}}{\partial\theta}\right|_{\tilde{\psi}} - in\Delta q(\tilde{\psi})\delta g^{(m)}\right] - i(\omega - n\omega_{d\tilde{\psi}}^\phi)\delta g^{(m)} \right\} \tag{9}$$

with corrections of order $\omega_d^\psi\omega_d^\phi\beta(\partial\delta g/\partial\tilde{\psi})/\dot{\theta}_0$, and where the toroidal drift is defined

$$\omega_{d\tilde{\psi}}^\phi = -\left[\boldsymbol{v}_d\cdot\boldsymbol{\nabla}\phi - q\boldsymbol{v}_d\cdot\boldsymbol{\nabla}\theta + \dot{\theta}_0(\psi-\tilde{\psi})\frac{dq}{d\psi}\right]. \tag{10}$$

Operating $\oint d\theta/\dot{\theta}$ on Eq. (9), and applying the boundary conditions of g for passing and trapped particles naturally introduces the (resonance) combination $D = \omega + p\sigma n\Delta q(\tilde{\psi})\omega_b - n\left\langle\omega_{d\tilde{\psi}}^\phi\right\rangle$, with σ the sign of $v_\parallel$,

$$\omega_b = \frac{2\pi}{\oint\frac{d\theta}{|\dot{\theta}|}} \quad \text{and} \quad \left\langle\omega_d^\phi\right\rangle = \frac{\omega_b}{2\pi}\oint\frac{d\theta\,\omega_d^\phi}{|\dot{\theta}|}$$

and $p=0$ for trapped particles, and $p=1$ for passing particles. Finally, a local dispersion relation should be written in terms of the flux label ψ rather than $\tilde{\psi}$. Noting that $\langle Fv_\parallel/\Omega_c\rangle = 0$ for trapped particles, one obtains the resonance term

$$D = \omega + p\sigma n\Delta q(\psi)\omega_b - n\left[\left\langle\omega_{d\psi}^\phi\right\rangle + p\omega_{d\psi}^\phi(\theta)\right] \tag{11}$$

where

$$\left\langle\omega_{d\psi}^\phi\right\rangle = -\left\langle\boldsymbol{v}_d\cdot\boldsymbol{\nabla}\phi + q\boldsymbol{v}_d\cdot\boldsymbol{\nabla}\theta - \dot{\theta}_0\left(\frac{Fv_\parallel}{\Omega_c} - \left\langle\frac{Fv_\parallel}{\Omega_c}\right\rangle\right)\frac{dq}{d\psi}\right\rangle \tag{12}$$

and

$$\omega_{d\psi}^\phi(\theta) = -\frac{dq}{d\psi}\omega_b\left(\frac{Fv_\parallel}{\Omega_c} - \left\langle\frac{Fv_\parallel}{\Omega_c}\right\rangle\right), \tag{13}$$

i.e. the transit average of Eq. (13) is zero. The drift term of Eq. (12) is identical to that used in Ref. [8] for resonant trapped and passing electrons, while in Ref. [5] the drift term employed is almost the same as Eq. (12) except for a different numerical coefficient in front of the last term in Eq. (12). It does not appear that the effect of the additional poloidally dependent term $\omega_{d\psi}^\phi(\theta)$ of Eq. (13) has been considered.

Finally, it is noted that the equilibrium electric field simply shifts the drift frequency by the toroidal plasma rotation frequency Ω_Φ associated with the electric field. Denoting subscript 'm' as magnetic (as opposed to electric), it follows that

$$\omega_d^\phi = \omega_{md}^\phi + \Omega_\Phi \ , \text{ with } \ \Omega_\Phi = -\frac{d\Phi}{d\psi}$$

It is also useful to write the toroidal drift in terms of the longitudinal invariant

$$\mathcal{J} = \oint v_\parallel dl$$

since this permits straightforward transformation between coordinates. Kadomstev [12] has shown that for trapped particles it is possible to write the bounce averaged toroidal drift entirely (and exactly [13]) in terms of variations in $\mathcal{J}$. The last term in Eq. (12) for passing particles is not included in Kadomstev's definition, and neither is the passing particle term of $\omega_{d\psi}^\phi(\theta)$. Nevertheless,

$$\left\langle\omega_{d\psi}^\phi\right\rangle = \left\langle\omega_{md\psi}^\phi\right\rangle + \Omega_\Phi \tag{14}$$

with

$$\left\langle \omega^{\phi}_{md\psi} \right\rangle = \frac{m}{Ze}\frac{\partial \mathcal{J}/\partial\psi\mid_{\mathcal{E}}}{\partial \mathcal{J}/\partial\mathcal{E}\mid_{\psi}} - \frac{dq}{d\psi}\omega_b \left\langle \frac{Fv_{\parallel}}{\Omega_c} \right\rangle \quad (15)$$

where $\mathcal{E} = \mathcal{K} - eZ\Phi/m = v^2/2$, and it is reiterated that the last term is zero for trapped particles.

B. The perturbed Lagrangian for MHD perturbations

In this section the perturbed Lagrangian contribution $\delta L^{\psi} = Ze\xi^{\psi}\omega^{\phi}_{d0}$ (using Eq. (5)) is evaluated for MHD-like fully electromagnetic perturbations. If MHD perturbations are assumed, the parallel electric field is zero. Moreover, the remaining perturbed electric potential is simply due to the equilibrium electric field observed in the moving frame, so that

$$\delta\phi = -\boldsymbol{\xi}_{\perp}\cdot\boldsymbol{\nabla}\Phi = -\xi^{\psi}\frac{d\Phi}{d\psi}.$$

Thus the electric potential does not appear in δL (neither $\delta\phi$ nor Φ). Hence the direct effect of $\boldsymbol{E}\times\boldsymbol{B}$ driven toroidal rotation does not enter into the interacting Lagrangian [14]. This result even holds for Sonic amplitude flows when the displacement is defined in the appropriate moving frame [15].

Regarding finite beta effects in the Lagrangian, it is noted that low frequency MHD perturbations do not allow compression of the magnetic field (no compressional Alfven waves), which requires that $\boldsymbol{\nabla}\cdot\boldsymbol{\xi}_{\perp} + 2\boldsymbol{\xi}_{\perp}\cdot\boldsymbol{\kappa} = 0$ and hence,

$$\delta B_{\parallel} = \frac{\xi_{\psi}}{B}\frac{dP}{d\psi}.$$

It is also seen from Eq. (5) and Eq. (10) that ω^{ϕ}_{d0} should be absent of the shear terms in ω^{ϕ}_{d}. This is represented by dividing the longitudinal invariant by q prior to taking variations (together with a correction of the order $\epsilon^2 dq/d\psi$). With all of these results it is clear that on ignoring the drift variation of ξ^{ψ}, the bounce averaged Lagrangian $\langle\delta L^{\psi}\rangle = Ze\xi^{\psi}\left\langle\omega^{\phi}_{d0}\right\rangle$ with

$$\left\langle \omega^{\phi}_{d0} \right\rangle = \frac{m}{Ze}\left\{\frac{\partial(\mathcal{J}/q)/\partial\psi\mid_{\mathcal{E}}}{\partial(\mathcal{J}/q)/\partial\mathcal{E}\mid_{\psi}} + \frac{1}{q}\frac{dq}{d\psi}\left\langle v_{\parallel}^2\left(1-\left[\frac{F}{RB}\right]^2\right)\right\rangle\right\} - \frac{\mu}{\Omega_c}\frac{dP}{d\psi}, \quad (16)$$

where

$$\langle X\rangle = \oint\frac{d\theta\,X}{\dot\theta}\bigg/\oint\frac{d\theta}{\dot\theta} = \oint\frac{dl\,X}{v_{\parallel}}\bigg/\oint\frac{dl}{v_{\parallel}}.$$

By also noting that the pressure gradient term exactly cancels a term in $\partial(\mathcal{J}/q)/\partial\psi$ due to the diamagnetic effect [1] on the toroidal field (approximately represented by the second term in Eq. (9) of Ref. [2]), the conclusion of this section is that the radial contribution to the perturbed Lagrangian δL^{ψ} is proportional to the toroidal drift precession in the absence of the equilibrium electric field, the direct effect of magnetic shear and diamagnetic effect on the toroidal magnetic field (note it will be seen later that the small shear term $dq/d\psi\left\langle v_{\parallel}^2[1-(F/RB)^2]\right\rangle$ is exactly cancelled by a weak shear dependent term in $\partial(\mathcal{J}/q)/\partial\psi$).

Finally, it is convenient to similarly break the total bounce averaged toroidal precession into terms that are absent of the direct effect of magnetic shear (indirect effects include the impact of shear in the Shafranov shift, and flux surface shaping penetration), and terms that depend on the shear. Hence it is clear that,

$$\left\langle \omega^{\phi}_{md\psi} \right\rangle = \frac{m}{Ze}\left\{\frac{\partial(\mathcal{J}/q)/\partial\psi\mid_{\mathcal{E}}}{\partial(\mathcal{J}/q)/\partial\mathcal{E}\mid_{\psi}} + \frac{1}{q}\frac{dq}{d\psi}\left\langle v_{\parallel}^2\left(1-\left[\frac{F}{RB}\right]^2\right)\right\rangle\right\} + \left\langle\omega^{\phi}_{mds}\right\rangle. \quad (17)$$

where $\left\langle\omega^{\phi}_{mds}\right\rangle$ represents the shear contribution to the orbit averaged magnetic drift precession:

$$\left\langle\omega^{\phi}_{mds}\right\rangle = \frac{1}{q}\frac{dq}{d\psi}\frac{m}{eZ}\left\{\left\langle\left[\frac{Fv_{\parallel}}{RB}\right]^2\right\rangle - q\omega_b F\left\langle\frac{v_{\parallel}}{B}\right\rangle\right\}. \quad (18)$$

C. Equilibrium distribution function

The perturbed distribution function is seen (Eqs. (1) and (2)) to depend on partial derivatives of the equilibrium distribution function F with respect to constants of motion $\mathcal{E}$, μ and $\tilde\psi$ (note $\mathcal{E}$ instead of $\mathcal{K}$ via using the Doppler shift associated with the equilibrium toroidal rotation Ω_{Φ} due to the equilibrium electric potential Φ). These derivatives acting on F can be expanded about the lowest order approximate equilibrium distribution function $F_0(\psi,\mathcal{E},\mu)$. Keeping leading order finite orbit width corrections gives:

$$\left.\frac{\partial F}{\partial P_{\phi}}\right|_{\mathcal{E},\lambda} = \frac{m}{Ze}\left.\frac{\partial F_0}{\partial\psi}\right|_{\mathcal{E},\lambda}(1+\Delta F_{P_{\phi}}) \text{ with } \Delta F_{P_{\phi}} = -\frac{\partial\psi_0}{\partial\psi} + \Delta\psi\left(\frac{\partial F_0}{\partial\psi}\right)^{-1}\frac{\partial^2 F_0}{\partial\psi^2}$$

$$\left.\frac{\partial F}{\partial \mathcal{E}}\right|_{P_\phi,\lambda} = \left.\frac{\partial F_0}{\partial \mathcal{E}}\right|_{\psi,\lambda}(1+\Delta F_{\mathcal{E}}) \text{ with } \Delta F_{\mathcal{E}} = \left(\frac{\partial F_0}{\partial \mathcal{E}}\right)^{-1}\left(-\frac{\partial \psi_0}{\partial \mathcal{E}}\frac{\partial F_0}{\partial \psi} + \Delta\psi \frac{\partial^2 F_0}{\partial \mathcal{E}\partial \psi}\right)$$

$$\left.\frac{\partial F}{\partial \lambda}\right|_{P_\phi,\mathcal{E}} = \left.\frac{\partial F_0}{\partial \lambda}\right|_{\psi,\mathcal{E}}(1+\Delta F_{\lambda}) \text{ with } \Delta F_{\lambda} = \left(\frac{\partial F_0}{\partial \lambda}\right)^{-1}\left(-\frac{\partial \psi_0}{\partial \lambda}\frac{\partial F_0}{\partial \psi} + \Delta\psi \frac{\partial^2 F_0}{\partial \lambda\partial \psi}\right)$$

where $\Delta\psi = \hat{\psi} - \psi = Fv_\parallel/\Omega_c - \psi_0$. Clearly, it remains to find a definition for ψ_0 that is consistent with neoclassical theory. To simplify the analysis, an energetic particle population is considered which is isotropic in pitch angle, or weakly anisotropic. As described in Ref. [9], energetic particles drag on both background electrons and background ions. When the fast particle velocity is larger than v_c then drag on the electrons dominate drag on the background ions, and vice-versa if $v < v_c$. Pitch angle scattering of energetic particles on the background ions is characterised by the velocity v_b, so that for $v_b \gg \{v, v_c\}$ pitch angle scattering dominates over drag, while drag dominates for $v_b \ll \{v, v_c\}$. Solutions to the Fokker-Plank equation for the equilibrium distribution function of Eqs. (6) and (7) are obtained via the equation

$$\left\langle C\left\{\left(\frac{Fv_\parallel}{\Omega_c} - \psi_0\right)\frac{\partial F_0}{\partial \psi}\right\}\right\rangle = 0,$$

where $C\{\}$ is the Fokker-Planck operator, which yields $\psi_0 = 0$ for trapped particles, while passing particles [9],

$$v_b^3 \frac{\partial F_0}{\partial \psi}\frac{\partial}{\partial \lambda}\left[\lambda\left(1 - \frac{1}{v}\frac{\left\langle v_\parallel^2/B\right\rangle}{\left\langle v_\parallel/B\right\rangle}\frac{\partial}{\partial \lambda}\frac{\mathcal{P}}{B_0}\right)\right] = \frac{\partial}{\partial v}\left\{(v^3+v_c^3)v\frac{\partial F_0}{\partial \psi}\left[1 - \frac{\mathcal{P}}{B_0}\frac{\partial}{\partial \lambda}\left(\frac{1}{v}\frac{\left\langle v_\parallel^2/B\right\rangle}{\left\langle v_\parallel/B\right\rangle}\right)\right]\right\} \quad (19)$$

where $\lambda = \mu/\mathcal{E}$ and $\mathcal{P}$ coincides with P in Ref. [9] so that

$$\frac{\mathcal{P}}{B_0} = -2\psi_0\frac{\Omega_c}{vFB}.$$

The main interest in this paper are the limiting solutions for $v_b = 0$ and $v_b \to \infty$. For alpha particles and ICRH ions one may assume the drag-only solution where pitch angle scattering can be legitimately neglected for the tail of the distribution. Thus taking $v_b = 0$ in Eq. (19) yields

$$\psi_0 = \frac{FB}{\Omega_c}\left\langle\frac{v_\parallel}{B}\right\rangle. \quad (20)$$

This is a particularly convenient result since for this case $\langle\psi\rangle = \hat{\psi}$, i.e. $\hat{\psi}$ represents the orbit time averaged radial position of the particle, just as it does for trapped particles (for which $\psi_0 = 0$). This definition of Eq. (20) for ψ_0 has notably been used for calculations of ICRH ion effects on kinetic-MHD instabilities in Refs. [16, 17]. It turns out that $\langle\psi\rangle = \hat{\psi}$ ensures the current associated with passing particle population is small. It can be shown that for large aspect ratio circular equilibria, the flux averaged parallel current density

$$j_\parallel = \frac{Ze}{2\pi}\int_{-\pi}^{\pi} d\theta \int dv^3 v_\parallel\left(\frac{Fv_\parallel}{\Omega_c} - \psi_0\right)\frac{\partial F_0}{\partial \psi} = -\frac{1}{B_\theta}\frac{dP}{dr}j_0$$

yields $j_0 = 0.43\epsilon^{3/2}(1 - 2\epsilon^{1/2} + \epsilon)$ for passing particles, and $j_0 = 1.2\epsilon^{3/2}(1 - 0.3\epsilon)$ for trapped particles. Here B_θ is the poloidal magnetic field.

For thermal ion populations in the banana regime, or for energetic electron distributions, an appropriate limiting solution of Eq. (19) would be $v_b \to \infty$ where pitch angle scattering dominates. This yields,

$$\psi_0(\lambda) = \frac{FB}{\Omega_c}\mathcal{E}\int_\lambda^{1/B_{max}} d\lambda' \frac{\left\langle v_\parallel/B\right\rangle}{\left\langle v_\parallel^2/B\right\rangle}, \quad (21)$$

for $\lambda < 1/B_{max}$. For a large aspect ratio circular tokamak this yields $j_0 = 1.46\epsilon^{1/2}$. This is the well known bootstrap current in neoclassical theory [18], and the factor $j_0 = 1.46\epsilon^{1/2}$ coincides exactly with the bootstrap current calculated in Ref. [19] for ECH populations in the isotropic and Lorentz limit. For the definition of Eq. (21) the parameter $\hat{\psi}$ is no longer identical to $\langle\psi\rangle$ for passing particles.

III. AXISYMMETRIC TOROIDAL EQUILIBRIUM EXPANSION

The toroidal drift, the perturbed lagrangian and the bounce frequency are now obtained using an expansion of the magnetic equilibrium. This enables a separation of the physical effects of shaping, Shafranov shift, finite beta, magnetic shear etc. This is undertaken by employing a new coordinate system with poloidal angle ω that does not have the straight field line property. It is also convenient to define the Jacobian in terms of a radial coordinate r, i.e. $J_{r,\omega} = |\nabla r \times \nabla\omega \cdot \nabla\phi|^{-1}$, so that $J_{r,\omega} = \psi' J_{\psi,\omega}$ where $J_{\psi,\omega} = |\nabla\psi \times \nabla\omega \cdot \nabla\phi|^{-1}$ and $\psi' = |\nabla\psi| = d\psi/dr$. From Eq. (3) one has

$$\boldsymbol{B} = F(\psi)\nabla\phi + \psi'\nabla r \times \nabla\phi = B_t\hat{e}_\phi + B_p\hat{e}_p$$

with $B_t = F/R$ the toroidal field strength, and $B_p = \psi'/R$ the poloidal field strength. The safety factor q is defined in terms of this Jacobian as

$$q = \frac{F(\psi)}{2\pi\psi'}\int_0^{2\pi} d\omega \frac{d\phi}{d\omega} = \frac{F(\psi)}{2\pi\psi'}\int_0^{2\pi} d\omega \frac{J_{r,\omega}}{R^2}. \quad (22)$$

Furthermore the safety factor is forced to satisfy the following on all flux surfaces without approximation:

$$q = \epsilon \frac{B_t}{B_p} = \epsilon \frac{F}{\psi'} \tag{23}$$

which is convenient because it coincides exactly with the result $\psi' = \epsilon F/q$ obtained from the straight field line system ψ, θ, ϕ of the previous section. Here $\epsilon = r/R_0$ and $R_0 = R(r = 0)$. The flux surfaces are described by the expansion

$$\begin{aligned} R &= R_0 + r\cos\omega - \Delta(r) + \sum_{m=2}^{\infty} S_m(r)\cos(m-1)\omega \\ &\quad + P(r)\cos\omega \qquad (24) \\ Z &= r\sin\omega - \sum_{m=2}^{\infty} S_m(r)\sin(m-1)\omega \\ &\quad - P(r)\sin\omega, \qquad (25) \end{aligned}$$

where the orderings $\Delta/R_0 \sim S_m/R_0 \sim P/r \sim \epsilon^2$ are formally assumed in the expansion that follows. S_2 is a measure of elongation and S_3 is a measure of triangularity etc (Δ is the Shafranov shift). The higher order parameter P relabels the magnetic surfaces [20]. A convenient definition of it is now given. Equality of the two definitions of $q(r)$ in Eqs. (22) and (23) yields

$$2\pi\epsilon = \int_{-\pi}^{\pi} d\omega\, \frac{J_{r,\omega}}{R^2}. \tag{26}$$

The Jacobian $J_{r,\omega}$ can be obtained in terms of radial derivatives in all the parameters in Eqs. (24) and (25) up to an order that includes $P(r)$. Then, substitution of $J_{r,\omega}$ into Eq. (26) yields the equality

$$\frac{P(r)}{R_0} = \epsilon\left(\frac{\epsilon^2}{8} + \frac{\Delta}{2R_0}\right) + \sum_m \frac{1-m}{2\epsilon}\left(\frac{S_m}{R_0}\right)^2$$

and substituting this back into the Jacobian gives:

$$J_{r,\omega} = rR_0(J_0 + J_1 + J_2) \tag{27}$$

with

$$\begin{aligned} J_0 &= 1 \\ J_1 &= (\epsilon - \Delta')\cos\omega + \sum_m \left((1-m)\frac{S_m}{r} + S'_m\right)\cos m\omega \\ J_2 &= -\frac{\epsilon}{2}[\epsilon + \Delta'(2+\cos 2\omega)] - 2\frac{\Delta}{R_0} + \\ &\quad \sum_m \left[\epsilon S'_m + \frac{S_m}{R_0}(1-m)\right]\cos\omega\cos m\omega + \\ &\quad \sum_m \frac{S_m}{R_0}\left[1 + (m-1)\frac{\Delta'}{\epsilon}\right]\cos(m-1)\omega, \qquad (28) \end{aligned}$$

which of course ensures that $\psi(r)' = \epsilon(F(r)/q(r))(1 + O(\epsilon^3))$. It follows that transformation between these coordinates and straight field line coordinates is obtained from equality of the volume element, i.e. $\int_\theta d\theta\psi' J_{\psi,\theta} = \int_\omega d\omega J_{r,\omega}$. Substituting $J_{\psi,\theta} = qR^2/F$ gives $\int_\theta d\theta (R/R_0)^2 = \int_\omega d\omega (J_0 + J_1 + J_2 + ..)$ which yields:

$$\theta = \omega - (\epsilon + \Delta')\sin\omega + \sum_m \left[(1-m)\frac{S_m}{r} + S'_m\right]\frac{\sin m\omega}{m} + O(\epsilon^2)$$

While stability studies [11] use such a transformation [11], the toroidal drift problem of concern here can be undertaken entirely in terms of the r, ω coordinates. Indeed the length increment is simply $dl = J_{\psi,\omega} B d\omega$, which enables calculation of the toroidal drift defined by Eqs. (17) and (18) via

$$\mathcal{J} = \oint d\omega\, v_\parallel J_{r,\omega} B/\psi' \quad \text{and} \quad \omega_b = 2\pi / \oint \frac{d\omega\, J_{r,\omega} B}{\psi' v_\parallel}$$

and

$$\langle X \rangle = \oint d\omega \frac{J_{r,\omega} B X}{\psi' v_\parallel} \bigg/ \oint d\omega \frac{J_{r,\omega} B}{\psi' v_\parallel}.$$

where use is also made of $\partial/\partial\psi = (\psi')^{-1}\partial/\partial r$. Thus it is seen that all that remains is a calculation of $B = (B_t^2 + B_p^2)^{1/2} = (F^2 + (\psi')^2)^{1/2}/R$ giving the expansion

$$\begin{aligned} B &= B_0\Bigg[1 - \epsilon\cos\omega + \epsilon^2\left(\cos^2\omega + \frac{1}{2q^2}\right) + \frac{\Delta}{R_0} + F_2 \\ &\quad - \sum_m \frac{S_m}{R_0}\cos(m-1)\omega + O(\epsilon^3)\Bigg] \qquad (29) \end{aligned}$$

where $F = R_0 B_0(1 + F_2(r) + O(\epsilon^3))$ and $F_2 = O(\epsilon^2)$ and $B_0 = B(r = 0)$. In the expressions that follow the equilibrium relation

$$rF'_2 = \frac{\epsilon}{q^2}\left(\frac{\alpha}{2} - \epsilon(2 - s)\right) \text{ with } \alpha = -q^2\frac{2R_0P'}{B_0^2}\ ,\ s = \frac{r}{q}\frac{dq}{dr}$$

has been assumed not least in order to simplify the expressions. Note that if the pressure gradient is steep only locally then $rF'_2 \sim \epsilon$ while still maintaining $F_2 \sim \epsilon^2$, which was the ordering assumed in Ref. [2], where the effect of $\alpha \sim 1$ on the toroidal drift was considered.

Another result required for the drift calculation is $\partial v_\parallel/\partial\psi = -(\mu/v_\parallel)\partial B/\partial\psi$. Now, $v_\parallel$ and the pitch angle $\lambda = \mu/\mathcal{E}$ can be written in terms of a convenient pitch angle y^2 for passing particles and $k^2 = 1/y^2$ for trapped particles. The pitch angles are defined over ranges $0 < y^2 < 1$ where the lower limit is for deeply passing particles for which $\mu = 0$ and the upper limit is for barely passing particles. Similarly $0 < k^2 < 1$ where $k^2 = 0$ is the deeply trapped limit, and $k^2 = 1$ is for barely trapped particles. In what follows, the effects of shaping beyond S_2 and S_3 are neglected. It is possible to show that for passing particles:

$$\lambda B_0 = y^2\frac{\overline{E}}{\mathcal{E}} \tag{30}$$

$$v_\parallel^2 = 4\overline{E}\left[\epsilon + \frac{S_2}{R_0}\right]\left[1 - y^2\left\{\sin^2\frac{\omega}{2} + X\sin^2\omega\right\}\right] \tag{31}$$

while for trapped particles:

$$\begin{aligned}\lambda B_0 &= \frac{\overline{E}}{\mathcal{E}}\\ v_\parallel^2 &= 4\overline{E}\left[\epsilon+\frac{S_2}{R_0}\right]\left[k^2-\left\{\sin^2\frac{\omega}{2}+X\sin^2\omega\right\}\right]\end{aligned}$$

where

$$X=\frac{1}{\epsilon+S_2/R_0}\left[\frac{S_3}{R_0}-\left(\epsilon+\frac{S_2}{R_0}\right)^2\right].$$

Also, for passing and trapped particles respectively:

$$\begin{aligned}\frac{\overline{E}}{\mathcal{E}} &= \frac{1}{y^2\left(1+F_2+\epsilon^2+\frac{\epsilon^2}{2q^2}+\frac{\Delta}{R_0}-\frac{S_3}{R_0}\right)+\left(\epsilon+\frac{S_2}{R_0}\right)(2-y^2)}\\ \frac{\overline{E}}{\mathcal{E}} &= \frac{1}{1+F_2+\epsilon^2+\frac{\epsilon^2}{2q^2}+\frac{\Delta}{R_0}-\frac{S_3}{R_0}+\left(\epsilon+\frac{S_2}{R_0}\right)(2k^2-1)}\end{aligned}$$

A. Analytic expansion of toroidal drift

With all of the above results it is possible to define the toroidal drift as

$$\left\langle\omega^\phi_{md\psi}\right\rangle=\frac{q\mathcal{E}}{rR_0\Omega_{c0}}\left(M+O(\epsilon^2)\right),$$

where for for passing particles:

$$M=\frac{\overline{E}}{\mathcal{E}}\frac{1}{\textcircled{F}}\left\{y^2\textcircled{A}+4\left[1+\frac{S_2}{r}\right]\left[\textcircled{B}+s\left(\textcircled{C}-\textcircled{D}\right)\right]\right\} \tag{32}$$

with $\Omega_{c0}=eZB_0/m$. While for trapped particles,

$$M=\frac{\overline{E}}{\mathcal{E}}\frac{1}{\textcircled{F}}\left\{\textcircled{A}+4\left[1+\frac{S_2}{r}\right]\left[\textcircled{B}+s\textcircled{C}\right]\right\}. \tag{33}$$

The bounce/transit frequency is given by

$$\omega_b=\frac{\sqrt{2\mathcal{E}}}{qR_0}\left(T+O(\epsilon^3)\right)$$

where

$$T=\frac{\pi}{2^{1/2}\textcircled{F}}\left[\frac{\overline{E}}{\mathcal{E}}(\epsilon+S_2/R_0)\right]^{1/2}. \tag{34}$$

In these expressions it can be shown that

$$\begin{aligned}\textcircled{A} = \;& I_2^- +\frac{2\epsilon-\alpha}{2q^2}I_1^- -\epsilon(I_1^-+I_5^-)-\frac{\Delta'}{2}(3I_1^-+I_5^-)\\ &+\left(S_2'-\frac{S_2}{r}\right)I_6^-+\left(S_3'-\frac{2S_3}{r}\right)I_8^-+S_2'I_2^-+S_3'I_5^-,\end{aligned}$$

$$\begin{aligned}\textcircled{B} = \;& \left(\frac{S_2}{r}-S_2'+rS_2''\right)I_5^+ +\left[2\left(\frac{S_3}{r}-S_3'\right)+rS_3''\right]I_7^+\\ &-r\Delta''I_2^+ +\left(\frac{\epsilon^2}{q^2}-\epsilon^2-\frac{3}{2}\epsilon\Delta'-\frac{\epsilon r\Delta''}{2}\right)I_1^+\\ &-\Delta'\left[\left(\frac{S_2}{r}-S_2'\right)I_2^+ +\left(\frac{2S_3}{r}-S_3'\right)I_5^+\right]\\ &+r\Delta''\left[\frac{S_2}{r}I_2^+ +\frac{2S_3}{r}I_5^+\right]\end{aligned}$$

$$\begin{aligned}\textcircled{C} = \;& I_1^+ -\Delta' I_2^+ -\left(\frac{S_2}{r}-S_2'\right)I_5^+ -\left(\frac{2S_3}{r}-S_3'\right)I_7^+\\ &-\left(\frac{\epsilon^2}{2q^2}(1+q^2)+\frac{\Delta}{R_0}+\frac{\epsilon\Delta'}{2}\right)I_1^+ +\Delta'\left(\frac{S_2}{r}I_2^+ +\frac{2S_3}{r}I_5^+\right)\end{aligned}$$

$$\begin{aligned}\textcircled{F} = \;& I_1^- -\Delta' I_2^- +\left(S_2'-\frac{S_2}{r}\right)I_5^- +\left(S_3'-\frac{2S_3}{r}\right)I_7^-\\ &+\left[\frac{\epsilon^2}{2}\left(\frac{1}{q^2}-1\right)-\frac{\Delta}{R_0}-\frac{\epsilon\Delta'}{2}\right]I_1^- +\frac{\Delta' S_2}{r}I_2^- +\frac{2\Delta' S_3}{r}I_5^-,\end{aligned}$$

where the definitions of $I_x^\pm$ are given in Appendix A. It is worth noting at this point that some of the shaping effects contained in $\textcircled{F}$ approximately vanish for vanishing magnetic shear, since (see Appendix B) in the absence of magnetic shear the Grad-Shafranov equation yields $S_2(r)\propto r$ and $S_3\propto r^2$. Consequently the shaping terms $S_2'-S_2/r$ and $S_3'-2S_3/r$ measure the combined effect of shaping and magnetic shear. Such terms appear also in $\textcircled{A}$, $\textcircled{B}$ and $\textcircled{C}$ (the shaping terms $(m-1)(S_m/r-S_m')+S_m''=0$ for $s=0$). These shaping effects, neglected in earlier studies [21] of the toroidal drift, are leading order for $s\sim 1$. The S_2' and S_3' terms in $\textcircled{A}$ are leading order shaping effects on the toroidal drift if the shear is small. For the bounce/transit frequency, leading order shaping effects exist in $\textcircled{F}$ also through the shaping dependence in X. Finally, it can be shown that

$$\textcircled{D}=\frac{\pi^2}{4\textcircled{F}}\left[1-\frac{\epsilon^2}{2}-\epsilon\Delta'-\frac{2\Delta}{R_0}\right].$$

The poloidally varying contribution $\omega^\phi_{d\psi}(\theta)$ of Eq. (13) that appears in the resonant term D of Eq. (11) can also be easily calculated. It is given by,

$$\omega^\phi_{d\psi}(\theta)=\frac{q\mathcal{E}}{rR_0\Omega_{c0}}\left(\tilde{M}+O(\epsilon^2)\right)$$

where

$$\begin{aligned}\tilde{M}=\;&\frac{\overline{E}}{\mathcal{E}}\frac{4s}{\textcircled{F}}\left(1+\frac{S_2}{r}\right)\Bigg[\textcircled{D}-\frac{\pi}{2}\times\\ &\left(1+\epsilon\cos\omega-\frac{\epsilon^2}{2q^2}-\frac{\Delta}{R_0}+\sum_m\frac{S_m}{R_0}\cos(m-1)\omega\right)\\ &\left(1-y^2\left\{\sin^2\left(\frac{\omega}{2}\right)+X\sin^2\omega\right\}\right)^{1/2}\Bigg],\end{aligned} \tag{35}$$

where simple coordinate transformation allows $\tilde{M}$ to be written in terms of θ if required. For well passing particles this constitutes a very large poloidally varying contribution to the drift. In magnitude it is of the order of the well known effect of the shear on the moderately trapped particles.

The perturbed Lagrangian $\langle \delta L^{\psi} \rangle = Ze\xi^{\psi} \left\langle \omega_{d0}^{\phi} \right\rangle$ of Eq. (16) is obtained through:

$$\left\langle \omega_{d0}^{\phi} \right\rangle = \frac{q\mathcal{E}}{rR_0\Omega_{c0}} \left(L + O(\epsilon^2) \right)$$

where for passing particles

$$L = \frac{\overline{E}}{\mathcal{E}} \frac{1}{Ⓕ} \left\{ y^2 \left(Ⓐ + \frac{\alpha}{2q^2} I_1^- \right) + 4 \left[1 + \frac{S_2}{r} \right] Ⓑ \right\} \quad (36)$$

and for trapped particles

$$L = \frac{\overline{E}}{\mathcal{E}} \frac{1}{Ⓕ} \left\{ \left(Ⓐ + \frac{\alpha}{2q^2} I_1^- \right) + 4 \left[1 + \frac{S_2}{r} \right] Ⓑ \right\}. \quad (37)$$

Examination of Ⓐ and Ⓑ confirms that the perturbed Lagrangian is indeed independent of the explicit dependence of magnetic shear. Moreover, as mentioned earlier, it is seen that the leading order α term that exists in ω_d^{ϕ} (derived in Ref.[1], and seen here in Ⓐ) is cancelled in the Lagrangian. While the direct effects of pressure gradient and shear are cancelled in the Lagrangian, the indirect effects of shear and pressure gradient are very important, since they affect toroidicity and shaping. For example, the $r\Delta'' I_2^+$ term in Ⓑ, derived originally in Ref. [2], does not cancel. For large pressure P gradients such that $rP' \sim \epsilon^{-1}P$ the Grad Shafranov equation yields $r\Delta'' = \alpha$. In general, as mentioned earlier, the effect of magnetic shear affects the penetration of shaping and Shafranov shift, and hence the derivatives of S_m and Δ.

The quantity ψ_0 required for the equilibrium distribution function for passing ions is given by

$$\psi_0 = \frac{m}{eZ} \overline{E}^{1/2} R_0 \left(\epsilon + \frac{S_2}{R_0} \right)^{1/2} \frac{4}{\pi} Ⓓ Ⓗ \quad (38)$$

where Ⓗ $= 1$ for the equilibrium distribution appropriate for alpha particles and ICRH ions (i.e. for $v_b = 0$ giving Eq. (20). In contrast, for an equilibrium distribution appropriate for thermal ions in the banana regime, or for superthermal electrons one obtains a more complicated expression consistent with Eq. (21) for which $v_b \to \infty$. In general:

$$Ⓗ = 1 \qquad \text{for } v_b = 0$$

$$Ⓗ = \frac{(1+F_2)Ⓕ}{2} \left(\frac{\mathcal{E}}{\overline{E}} \right)^{1/2} \int_{y^2}^{1} \frac{dy^2}{Ⓖ} \left(\frac{\overline{E}}{\mathcal{E}} \right)^{3/2} \qquad \text{for } v_b \to \infty$$

where

$$Ⓖ = I_1^+ + (\epsilon - \Delta') I_2^+ - \left(\frac{S_2}{r} - S_2' \right) I_5^+ - \left(2\frac{S_3}{r} - S_3' \right) I_7^+ - \left(\frac{\epsilon^2}{2} + \epsilon\Delta' + \frac{2\Delta}{R_0} \right) I_1^+ - \frac{\epsilon\Delta'}{2} I_5^+ + (\epsilon + \Delta') \frac{S_2}{r} I_2^+ + (\epsilon + 2\Delta') \frac{S_3}{r} I_5^+ + \epsilon \left(S_2' - \frac{S_2}{r} \right) I_6^+ + \epsilon \left(S_3' - 2\frac{S_3}{r} \right) I_8^+$$

Finally, note that while Ⓐ and Ⓑ are required only to $O(\epsilon)$, Ⓒ and Ⓓ are required at the next order in the deeply passing limit, where formally larger terms cancel or integrate to zero.

B. Deeply trapped limit

In the deeply trapped limit $k^2 = 0$ giving Ⓑ $=$ Ⓒ $= 0$. Meanwhile Ⓐ and Ⓕ are simplified using $I_1^- = I_2^- = I_5^- = I_6^- = I_7^- = I_8^- = (\pi/2)/\sqrt{1+4X} \approx (\pi/2)(1-2X)$, which introduces additional leading order triangularity effects and toroidal corrections in the bounce frequency. It is now easy to show that the deeply trapped limit of the normalised toroidal drift is:

$$M = 1 - \epsilon \left(1 - \frac{1}{q^2} \right) - \frac{\alpha}{2q^2} - \Delta' + S_2' + S_3' + O(\epsilon^2) \quad (39)$$

which agrees with the result obtained in Ref. [21], except for the toroidal terms, $\epsilon(1 - 1/q^2)$, that were neglected in Ref. [21]. These toroidal effects reduce the deeply trapped drift for $q > 1$, or increase the deeply trapped drift for $q < 1$. The toroidal effect of $\Delta' \approx \epsilon(\beta_p + l_i/2)$ reduces the deeply trapped toroidal drift. The effect of shaping can be seen through conventional definitions of shaping (elongation κ and triangularity δ) via (see Appendix B)

$$\frac{S_2}{r} = -\frac{\kappa - 1}{\kappa + 1} \quad \text{and} \quad \frac{S_3}{r} = \frac{\delta}{4}$$

and for small shear $S_2' = S_2/r$ and $S_3' = 2S_3/r$. Thus conventional vertical elongation reduces, and conventional outward triangularity increases, the deeply trapped drift.

Meanwhile, the normalised perturbed Lagrangian is identical to M above but without the α term. Finally, the bounce frequency in the deeply trapped limit is

$$T = \sqrt{2\epsilon} \left[1 - \frac{3}{2}\epsilon + \Delta' + \left(\frac{S_2}{r} - S_2' \right) + \left(\frac{2S_3}{r} - S_3' \right) + \frac{2S_3}{r} + \frac{S_2}{2r} \right] + O(\epsilon^2) \quad (40)$$

where the shaping terms in brackets cancel for vanishing shear, while the others indicate that elongation reduces the bounce frequency, while triangularity increases it. Toroidal effects that enter via Δ' increases T.

C. Barely passing/trapped limit

While the bounce/transit frequency vanishes at the passing trapped boundary $y^2 = k^2 = 1$, the toroidal drift

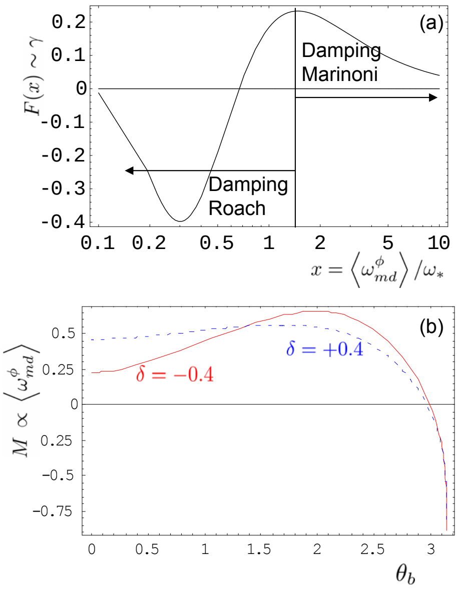

FIG. 1: (a) A plot of $\mathrm{F} = x^{-3/2}(3/2 - 1/x)\exp(-1/x)$ where $x = \left\langle \omega_{md}^{\phi} \right\rangle / \omega_*$. Maximum growth occurs for $x \approx 1$. In (b) the normalised toroidal drift M is plotted with respect to bounce angle for equilibria with positive triangularity ($\delta = 0.4$ blue dotted) and negative triangularity ($\delta = -0.4$ red solid).

frequency is reversed, and the magnitude of M is order unity. At the boundary, Ⓐ and Ⓕ are infinitely larger than Ⓑ, Ⓒ and Ⓓ. Meanwhile, $I_2^-/I_1^- = I_6^-/I_1^- = I_7^-/I_1^- = -1$ and $I_5^-/I_1^- = I_8^-/I_7^- = 1$ finally gives at the trapped-passing boundary

$$M = -1 - \epsilon\left(1 - \frac{1}{q^2}\right) - \frac{\alpha}{2q^2} - \Delta' - S_2' + S_3' + O(\epsilon^2).$$

Physical effects that assist reversal in the direction of the drift at the boundary include ϵ (if $q > 1$), α and Δ'. In contrast both conventional outward triangularity and conventional vertical elongation act to prevent deep reversal of the drift. This is consistent with the earlier comment that electron fishbones appear to be more frequently observed in circular tokamaks than conventional shaped tokamaks. Circular tokamaks also tend to have poorer confinement, and hence smaller α and Δ', which further reduces the number of reverse trapped particles and the fishbone drive.

While the effect of triangularity acts to increase the drift at both the deeply and barely trapped limits, it is seen that for intermediate trapped pitch angle, the triangularity reduces the toroidal drift. This is in agreement with simulations and TCV experiments examining the impact of plasma shaping on TEMs [7]. Here it was argued that negative triangularity would favourably reduce TEM growth rate via an increase in the toroidal drift frequency (at intermediate pitch angle), while positive triangularity would increase TEM growth rate via a decrease in the toroidal drift. This argument can be seen via the growth rate for the TEM [22]:

$$\gamma \sim \int \frac{d\lambda}{v_\parallel}\mathrm{F}(x) \;\; \text{with} \;\; \mathrm{F} = x^{-3/2}\left(\frac{3}{2} - \frac{1}{x}\right)\exp\left(-\frac{1}{x}\right)$$

where $x = \left\langle \omega_{md}^{\phi} \right\rangle / \omega_*$ and $\omega \sim \omega_*$ has been assumed. In Fig. 1 (a) it is seen that maximum growth rates occur for $x \approx 1$. Damping in Ref. [22] was discussed in terms of $x < 1$ which is clearly robust, especially when particles are reverse trapped (no resonance possible). In contrast, the damping considered in Ref. [7] appears to be related to $x > 1$, which occurs more easily for negative triangularity. In Fig. 1 (b) the trapped drift precession of Eq. (33) is plotted with respect to bounce angle (Eq. (A1)) for positive triangularity ($\delta = 0.4$) and negative triangularity ($\delta = -0.4$), while other parameters are taken to be standard values defined in Section IV. As a final point, both ψ_0 and $\tilde{M}$ are zero for barely passing particles, just as they are for all trapped particles.

D. Deeply passing limit

In the deeply passing limit $y^2 = 0$ the Ⓐ term vanishes. Meanwhile, $I_1^+ = I_1^- = \pi/2$, while all the other I terms are zero. This leads to the normalised transit frequency:

$$T = 1 + \frac{\epsilon^2}{2}\left(1 - \frac{1}{q^2}\right) + \frac{\epsilon\Delta'}{2} + \frac{\Delta}{R_0} + O(\epsilon^3)$$

so that toroidal effects are weak corrections to the standard result $T = 1$. Toroidal, shaping and magnetic shear corrections to the magnetic drift are at least an order of magnitude larger than for the corresponding effects on the transit frequency. In the deeply passing limit the drift is given by

$$M = 2\epsilon\left(\frac{1}{q^2} - 1\right) - 3\Delta' - r\Delta'' - \epsilon s + O(\epsilon^2) \qquad (41)$$

Note that the effect of shaping has disappeared, but a small term proportional to the magnetic shear remains. The result agrees with the deeply passing circular cross section calculation of [4], except that the analytic expressions of Ref. [4] did not address the effect of shaping, nor of the magnetic shear. Clearly, for $q > 1$ and positive shear, all the terms in M act so as to deeply reverse the toroidal drift frequency. Thus, despite most of the terms being formally order ϵ, the combination of effects in practice ensures that the amplitude of the toroidal drift frequency of passing particles is similar to that of deeply trapped particles. Moreover, as mentioned before, $r\Delta'' = \alpha$ for strong pressure gradients, and therefore, for $q > 2^{-1/2}$, the $r\Delta''$ term for deeply passing particles is larger than the toroidal magnetic well term (the α term) derived by Rosenbluth and Sloan [1] for trapped particles. Nevertheless, it should be kept in mind that the toroidal drift for deeply passing particles is typically important in the drift kinetic equation only close to a rational surface where $\Delta q\omega_b$ is not overly dominant, or for very energetic ions for which the ratio $\omega_b/\omega_{md}^{\phi}$ is reduced. It is thought that electron fishbones could exist [8] in equilibria where Δq is small over a large extent of the plasma, and so the deeply passing limit of the drift could be relevant for electrons too.

The poloidally varying contribution $\omega_{d\psi}^{\phi}(\theta)$ of Eq. (13) that appears in the resonant term D of Eq. (11) is evaluated through $\tilde{M}$ as defined in Eq. (35). In the deeply passing limit $y^2 = 0$ one obtains

$$\tilde{M} = -s\left(2\cos\omega + \Delta' + 2\sum_m \frac{S_m}{r}\cos(m-1)\omega + O(\epsilon^2)\right),$$

which transit averages to zero. This oscillating contribution to the local resonance term $D(\psi)$ is larger in amplitude than any other contribution to D across all pitch angles if the shear $s \sim 1$.

The normalised perturbed Lagrangian is identical to the toroidal drift expressions without the magnetic shear:

$$L = 2\epsilon\left(\frac{1}{q^2} - 1\right) - 3\Delta' - r\Delta'' + O(\epsilon^2)$$

Thus it is seen that a strong pressure gradient effect $r\Delta'' \sim \alpha$ is retained in the Lagrangian for the deeply passing particles, while as has been seen, the direct effect of α was cancelled in the expression of the perturbed Lagrangian for the trapped particles. The fact that the Lagrangian is large in amplitude for deeply passing particles demonstrates that passing particles can contribute to kinetic corrections to MHD instabilities, providing the additional constraint $\Delta q\omega_b \sim \left\langle \omega_{md}^{\phi} \right\rangle$ is also met over the mode structure. That deeply passing particles can contribute kinetic corrections to MHD is in contrast to early statements made in seminal papers on the subject.

Finally the constant ψ_0 that defines the neoclassical equilibrium is considered for the deeply passing case, and for the choices $v_b = 0$ appropriate for energetic ion populations such as alpha's, and for $v_b \to \infty$ appropriate e.g. for electron distributions or thermal ions in the banana regime. From Eq. (38), and taking $y^2 = 0$ one obtains for $v_b = 0$:

$$\psi_0 = \frac{m}{eZ}(2\mathcal{E})^{1/2}R_0(1 + O(\epsilon^2)),$$

while for $v_b \to \infty$,

$$\psi_0 = \frac{m}{eZ}(2\mathcal{E})^{1/2}R_0\left(1 - \epsilon^{1/2} + \epsilon\left(1 - \frac{\pi}{4}\right) + O(\epsilon^{3/2})\right).$$

It turns out that the differences between these expressions has a large effect on $\Delta\psi = Fv_\parallel/\Omega_c - \psi_0$ for passing particles (as seen in Sec. II C both $\Delta\psi$ and ψ_0 appear in the drift kinetic equation). Again choosing $y^2 = 0$ one obtains for $v_b = 0$:

$$\Delta\psi = \frac{m}{eZ}(2\mathcal{E})^{1/2}R_0(\epsilon\cos\omega + O(\epsilon^2))$$

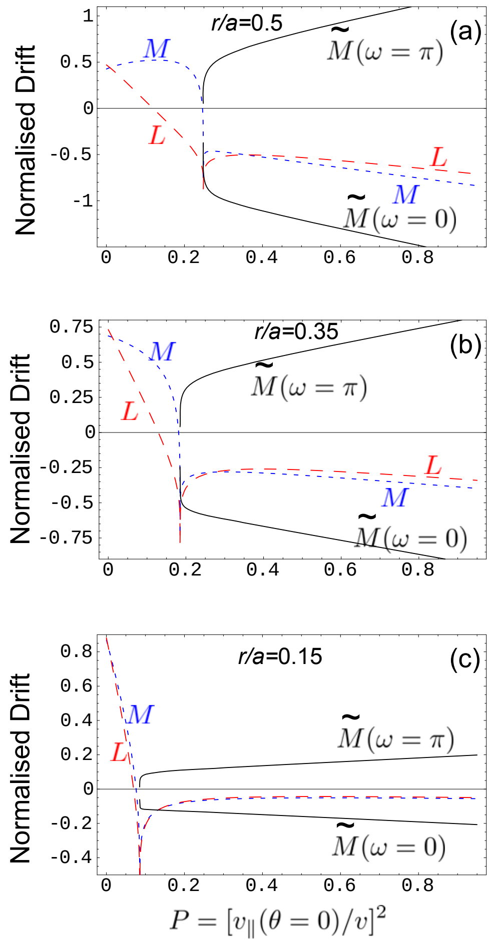

FIG. 2: Drift frequencies at various radial positions for standard tokamak equilibria ($\delta = 0.4$, $\kappa = 1.5$) with large pressure gradient around $r/a = 0.45$. Shown are the normalised Lagrangian L (red-dashed), the normalised drift precession frequency M (blue-dotted), and the poloidally varying contribution to the resonance term $\tilde{M}$ (black-solid) evaluated at $\omega = 0$ and $\omega = \pi$ (these two curves are approximately the maximum and minimum values of $\tilde{M}$).

which is purely oscillating. The case of $v_b \to \infty$ has an additional constant that is $\epsilon^{-1/2}$ larger:

$$\Delta\psi = \frac{m}{eZ}(2\mathcal{E})^{1/2}R_0\left(\epsilon^{1/2} - \epsilon\left(1 - \frac{\pi}{4}\right) + \epsilon\cos\omega + O(\epsilon^{3/2})\right)$$

IV. DRIFT PRECESSION AND BOUNCE/TRANSIT FREQUENCY OVER ARBITRARY PITCH ANGLE

In this section the drift and bounce/transit frequencies are evaluated across pitch angle space for tokamak equilibria defined with $q = 1 - \Delta q[1 - (r/r_1)^2]$, $r_1 = 0.25a$, $r_2 = 0.7a$ (where $\Delta q = 1/[1 - (r_2/r_1)^2]$), $\beta = 2P/B_0^2 = \beta_0[1 - \tanh(15(r - 0.4a)/R_0)/(1 - \tanh(-6a/15))]$ with $\beta_0 = 0.01$, $R_0/a = 3$, edge elongation $\kappa = 1.5$ and edge

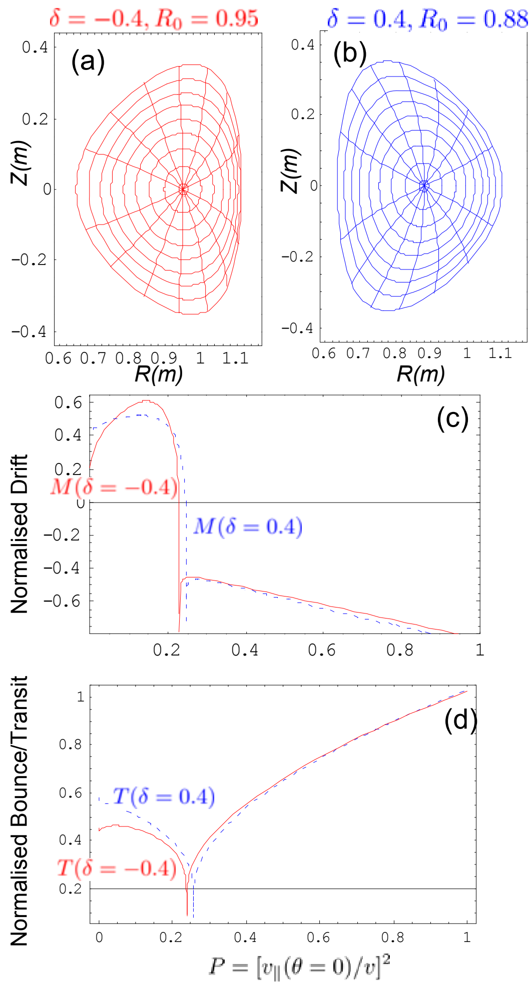

FIG. 3: Showing in (a) and (b) the grid in r, ω coordinates for TCV equilibria with respectively negative triangularity $\delta = -0.4$ and positive triangularity $\delta = 0.4$. In (c) the normalised precession drift M is plotted at mid radius $r/a = 0.5$ (red-solid line for $\delta = -0.4$, and blue-dotted for $\delta = 0.4$). Shown in (d) are the transit/bounce frequencies T for the two equilibria at mid-radius.

triangularity $\delta = 0.4$. It is now possible to examine the dependence of drift frequency and Lagrangian with respect to pitch angle for a typical equilibrium. The chosen pitch angle $P = (v_{\|}(\theta = 0)/v)^2$ can easily be written in term of k^2 or y^2:

$$y^2 = \frac{2(1-P)\left(\epsilon + \frac{S_2}{R_0}\right)}{P\left(1 - \epsilon - \frac{S_2}{R_0} - \frac{S_3}{R_0} + \frac{\Delta}{R_0} + F_2 + \epsilon^2 + \frac{\epsilon^2}{2q^2}\right)}.$$

In Fig. 2 the normalised drift frequencies are shown for three radial positions. At $r/a = 0.5$ the pressure gradient is large, and this is reflected in part by a diminished value of $\left\langle \omega^{\phi}_{md\psi} \right\rangle$ at the deeply trapped limit, and also a large negative value of $\left\langle \omega^{\phi}_{md\psi} \right\rangle$ at the deeply passing limit. Meanwhile, the impact of the effect of shear on the trapped particle drift is seen by comparing $\left\langle \omega^{\phi}_{md\psi} \right\rangle$ (i.e. M) with the Lagrangian, since the Lagrangian is independent of the direct effect of shear. It is seen that the Lagrangian, which measures the potential for wave-particle interaction, is larger in amplitude for passing particles than for trapped particles (at $r = 0.5a$). As r/a is reduced the effects of toroidicity and pressure diminish, and as a result the amplitude of the Lagrangian for passing particles is reduced. Examining the Lagrangian at the various radial positions, the strong impact of the pressure gradient and toroidicity on passing particles is seen, and the moderate impact of pressure and toroidicity on the toroidal drift of the deeply trapped particles (where effect of shear vanishes) is also seen. Moreover, the shear is reduced as r/a is reduced, and it is mainly for this reason that L and M become equivalent as r/a is reduced. Finally, also shown in Fig. 2 is the poloidally dependent contribution $\tilde{M}$ to the resonance term D. As noted earlier, the amplitude of $\tilde{M}$ for passing particles is expected to be larger than the bounce averaged normalised drift M when $s \sim 1$. By choosing $\omega = 0$ and $\omega = \pi$ it is possible to observe the approximate maximum and minimum values of $\tilde{M}$ (min/max with respect to ω) in the black solid curves in Fig. 2. The amplitude of $\tilde{M}$ is reduced as r/a is reduced due to the corresponding reduction in shear s ($s = 0.81$ at $r = 0.5a$, $s = 0.5$ at $r = 0.35a$ and $s = 0.12$ at $r = 0.15a$).

It is interesting to examine the impact of shaping on the toroidal drift and the bounce frequency for realistic TCV equilibria. For the positive triangularity case shown in Fig. 3 the equilibrium remains the same as in Fig. 2, but with the specific choice $R_0 = 0.88$. For the negative triangularity case (edge triangularity $\delta = -0.4$) the major radius of the magnetic axis is moved outwards in order to maintain the position of the outermost flux surfaces ($R_0 = 0.95$). The impact of triangularity is seen across all pitch angles at mid radius position $r/a = 0.5$. While the impact of triangularity on the trapped particles precession is significant (as also seen in Fig. 1), the impact on the drift precession of passing particles is weak. This is consistent with the deep passing limit of Eq. (41). The effect of shaping on the bounce frequency is considerable for trapped particles. The effect of triangularity is weak for deeply passing particles as expected.

Finally, to complete an examination into the effect of plasma cross section, Fig. 4 essentially repeats Fig. 3 but this time with vanishing triangularity, and two choices of elongation (vertical elongation, and circular cross section). It is found that once again the effect of elongation has a very strong impact on the trapped particle toroidal drift and a moderate effect on the bounce frequency. As expected from the deeply trapped limit for the toroidal drift of Eq. (39) the impact of elongation is a reduction of the drift. However, as expected from Eq. (40) the impact of shaping is more complicated for the bounce frequency due to shaping terms that are non-zero when there is also magnetic shear (the $mS_m/r - S'_m$ terms).

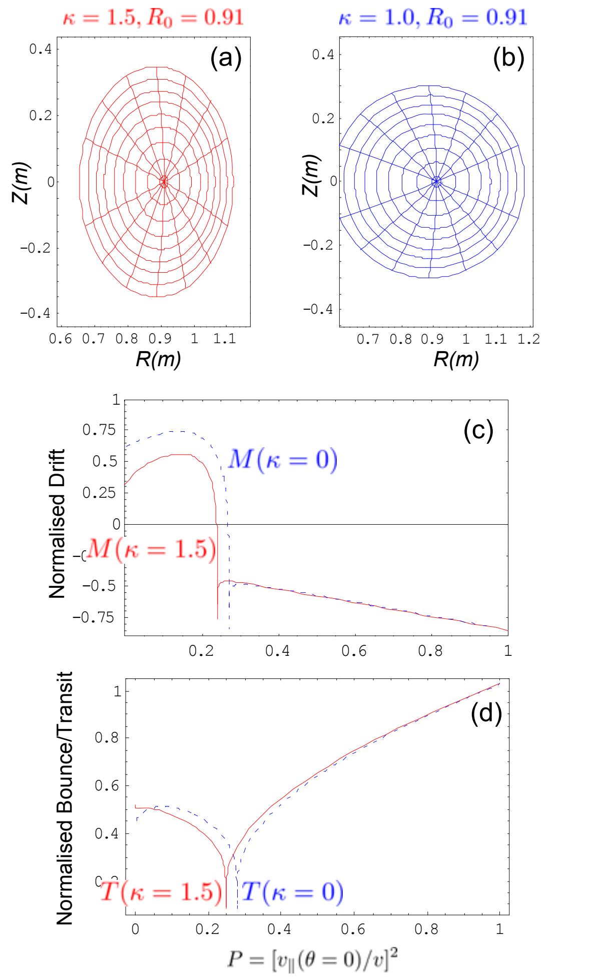

FIG. 4: Showing in (a) and (b) the grid in r, ω coordinates for TCV equilibria with respectively elongation $\kappa = 1.5$ and elongation $\kappa = 1.0$. In both case $\delta = 0$, so that case (b) is circular. In (c) the normalised precession drift M is plotted at mid radius $r/a = 0.5$ (red-solid line for $\kappa = 1.5$, and blue-dotted for $\kappa = 1.0$). Shown in (d) are the transit/bounce frequencies T for the two equilibria at mid-radius.

V. CONCLUSIONS

The drift kinetic equation has been expanded around a neoclassically resolved equilibrium distribution function for particles with long mean free path. The resulting toroidal drift is evaluated for shaped equilibria with finite beta effects. Where possible, analytic results are obtained in terms of physical parameters, and conclusions are drawn about the impact of the new physics on energetic particle driven modes. The work extends previous results to include magnetic shear and shaping for deeply passing particles, and yields a derivation of the toroidal drift of passing particles at other pitch angles to an ordering in ϵ higher than required for trapped particles. The impact of pressure gradients and toroidicty ensure that the toroidal drift of passing particles is comparable with that of trapped particles at mid radius in a conventional aspect ratio tokamak. Moreover, the impact of magnetic shear on the passing particle toroidal drift is felt most strongly through a poloidally dependent term in the resonance contribution to the drift kinetic equation. The effect of shaping on trapped particles is extended to include the combined effect of magnetic shear and plasma cross section shaping. This effect manifests itself via the way in which magnetic shear impacts on the penetration of the shaping from the plasma boundary. All of this work has required a consistent derivation of the drift and the bounce/transit frequency to higher order in ϵ across all pitch angles than has been undertaken previously.

Acknowledgements

A number of helpful discussions on neoclassical equilibria with S. Brunner and T. Vernay are acknowledged. This work, supported by the Swiss National Science Foundation, and by the European Communities under contract of Association between EURATOM and Confédération Suisse, was carried out within the framework of the European Fusion Development Agreement. The views and opinions expressed herein do not necessarily reflect those of the European Commission.

APPENDIX A: BOUNCE/TRANSIT AVERAGE INTEGRALS

The following general expressions are required for the toroidal drift for passing particles:

$$\begin{aligned}
I_1^{\pm} &= \frac{1}{4}\int_{-\pi}^{\pi} d\omega[1 - y^2(\sin^2(\omega/2) + X\sin^2\omega)]^{\pm\frac{1}{2}} \\
I_2^{\pm} &= \frac{1}{4}\int_{-\pi}^{\pi} d\omega\cos\omega[1 - y^2(\sin^2(\omega/2) + X\sin^2\omega)]^{\pm\frac{1}{2}} \\
I_5^{\pm} &= \frac{1}{4}\int_{-\pi}^{\pi} d\omega\cos 2\omega[1 - y^2(\sin^2(\omega/2) + X\sin^2\omega)]^{\pm\frac{1}{2}} \\
I_6^{\pm} &= \frac{1}{4}\int_{-\pi}^{\pi} d\omega\cos 2\omega\cos\omega[1 - y^2(\sin^2(\omega/2) + X\sin^2\omega)]^{\pm\frac{1}{2}} \\
I_7^{\pm} &= \frac{1}{4}\int_{-\pi}^{\pi} d\omega\cos 3\omega[1 - y^2(\sin^2(\omega/2) + X\sin^2\omega)]^{\pm\frac{1}{2}} \\
I_8^{\pm} &= \frac{1}{4}\int_{-\pi}^{\pi} d\omega\cos 3\omega\cos\omega[1 - y^2(\sin^2(\omega/2) + X\sin^2\omega)]^{\pm\frac{1}{2}}.
\end{aligned}$$

The following general expressions are required for the toroidal drift for trapped particles:

$$\begin{aligned}
I_1^{\pm} &= \frac{1}{4}\int_{-\theta_b}^{\theta_b} d\omega[k^2 - (\sin^2(\omega/2) + X\sin^2\omega)]^{\pm\frac{1}{2}} \\
I_2^{\pm} &= \frac{1}{4}\int_{-\theta_b}^{\theta_b} d\omega\cos\omega[k^2 - (\sin^2(\omega/2) + X\sin^2\omega)]^{\pm\frac{1}{2}} \\
I_5^{\pm} &= \frac{1}{4}\int_{-\theta_b}^{\theta_b} d\omega\cos 2\omega[k^2 - (\sin^2(\omega/2) + X\sin^2\omega)]^{\pm\frac{1}{2}}
\end{aligned}$$

$$I_6^{\pm} = \frac{1}{4}\int_{-\theta_b}^{\theta_b} d\omega \cos 2\omega \cos\omega [k^2 - (\sin^2(\omega/2) + X\sin^2\omega)]^{\pm\frac{1}{2}}$$
$$I_7^{\pm} = \frac{1}{4}\int_{-\theta_b}^{\theta_b} d\omega \cos 3\omega [k^2 - (\sin^2(\omega/2) + X\sin^2\omega)]^{\pm\frac{1}{2}}$$
$$I_8^{\pm} = \frac{1}{4}\int_{-\theta_b}^{\theta_b} d\omega \cos 3\omega \cos\omega [k^2 - (\sin^2(\omega/2) + X\sin^2\omega)]^{\pm\frac{1}{2}}$$

where the limit of integration $\theta_b = \omega(v_\| = 0)$ is the bounce angle:

$$\theta_b(k^2) = 2\arccos\left[\sqrt{\frac{-1+4X+\sqrt{(1+4X)^2-16Xk^2}}{8X}}\right], \tag{A1}$$

which reduces to $\theta_b = 2\arcsin k$ for $X = 0$. Now, non zero X is formally required for the higher order expansion obtained in this work, and indeed leading order triangularity effects in the deeply trapped expression for the bounce frequency arises in part from the effect of triangularity in X. In particular for $k = 0$, $I_1^- = I_2^- = I_5^- = I_6^- = I_7^- = I_8^- = (\pi/2)/\sqrt{1+4X} \approx (\pi/2)(1-2X)$. The effect of X disappears in deeply trapped, barely trapped and deeply passing limits of the toroidal drift, but appears at relevant order for other values of pitch angle. Nevertheless, taking $X = 0$ leads to expressions in terms of elliptic integrals of the first kind $K(y^2)$ and second kind $E(y^2)$. For passing particles in the limit $X = 0$:

$$I_1^+ = E(y^2)$$
$$I_2^+ = \frac{4(y^2-1)K(y^2) - 2(y^2-2)E(y^2)}{6y^2}$$
$$I_5^+ = \frac{16\left(y^4-3y^2+2\right)K(y^2) - 2\left(y^4-16y^2+16\right)E(y^2)}{30y^4}$$
$$I_6^+ = \frac{\left(-38y^6+204y^4-384y^2+256\right)E\left(y^2\right) + 4\left(31y^6-95y^4+128y^2-64\right)K\left(y^2\right)}{210y^6}$$
$$I_7^+ = \frac{\left(-6y^6+268y^4-768y^2+512\right)E(y^2) + 4\left(27y^6-155y^4+256y^2-128\right)K(y^2)}{210y^6}$$
$$I_8^+ = \frac{\left(-26y^8+784y^6-2832y^4+4096y^2-2048\right)E\left(y^2\right) + 8\left(41y^8-251y^6+594y^4-640y^2+256\right)K\left(y^2\right)}{630y^8}$$
$$I_1^- = K(y^2)$$
$$I_2^- = \frac{4E\left(y^2\right) + 2\left(y^2-2\right)K\left(y^2\right)}{2y^2}$$
$$I_5^- = \frac{16\left(y^2-2\right)E\left(y^2\right) + \left(6y^4-32y^2+32\right)K\left(y^2\right)}{6y^4}$$
$$I_6^- = \frac{2\left(19y^4-64y^2+64\right)E\left(y^2\right) + \left(15y^6-94y^4+192y^2-128\right)K\left(y^2\right)}{15y^6}$$
$$I_7^- = \frac{\left(92y^4-512y^2+512\right)E\left(y^2\right) + \left(30y^6-316y^4+768y^2-512\right)K\left(y^2\right)}{30y^6}$$
$$I_8^- = \frac{4\left(79y^6-542y^4+1152y^2-768\right)E\left(y^2\right) + \left(105y^8-1208y^6+4280y^4-6144y^2+3072\right)K\left(y^2\right)}{105y^8}.$$

For trapped particles ($X = 0$):

$$I_1^+ = E\left(k^2\right) + \left(k^2-1\right)K\left(k^2\right)$$
$$I_2^+ = \frac{1}{3}\left(\left(2k^2-1\right)E\left(k^2\right) - \left(k^2-1\right)K\left(k^2\right)\right)$$
$$I_5^+ = \frac{1}{15}\left(\left(-16k^4+16k^2-1\right)E\left(k^2\right) + \left(8k^4-9k^2+1\right)K\left(k^2\right)\right)$$
$$I_6^+ = \frac{1}{105}\left(\left(128k^6-192k^4+102k^2-19\right)E\left(k^2\right) + \left(-64k^6+104k^4-59k^2+19\right)K\left(k^2\right)\right)$$

$$
\begin{aligned}
I_7^+ &= \frac{1}{105}\left(\left(256k^6-384k^4+134k^2-3\right)E\left(k^2\right)+\left(-128k^6+208k^4-83k^2+3\right)K\left(k^2\right)\right)\\
I_8^+ &= \frac{1}{315}\left(\left(-1024k^8+2048k^6-1416k^4+392k^2-13\right)E\left(k^2\right)+\left(512k^8-1088k^6+804k^4-241k^2+13\right)K\left(k^2\right)\right)\\
I_1^- &= K\left(k^2\right)\\
I_2^- &= 2E\left(k^2\right)-K\left(k^2\right)\\
I_5^- &= \frac{1}{3}\left(\left(8-16k^2\right)E\left(k^2\right)+\left(8k^2-5\right)K\left(k^2\right)\right)\\
I_6^- &= \frac{1}{15}\left(2\left(64k^4-64k^2+19\right)E\left(k^2\right)+\left(-64k^4+72k^2-23\right)K\left(k^2\right)\right)\\
I_7^- &= \frac{1}{15}\left(\left(256k^4-256k^2+46\right)E\left(k^2\right)+\left(-128k^4+144k^2-31\right)K\left(k^2\right)\right)\\
I_8^- &= \frac{1}{105}\left(\left(1536k^6-2496k^4+1276k^2-211\right)K\left(k^2\right)-4\left(768k^6-1152k^4+542k^2-79\right)E\left(k^2\right)\right).
\end{aligned}
$$

APPENDIX B: EQUILIBRIUM COEFFICIENTS AND COORDINATE TRANSFORMATIONS

The Grad Shafranov equation can be solved for the coefficients employed for the drift calculations of this paper. Required profiles to be solved are $\Delta(r)$, $S_2(r)$, $S_3(r)$ and $F_2(r)$, and these are obtained in terms of chosen values R_0, B_0, $S_2(a)$, $S_3(a)$ (where $r = a$ is the edge radius) together with current and pressure profiles, or $q(r)$ and $\alpha(r)$. Assuming large aspect ratio one obtains lowest order solutions by inspection of Fourier coefficients of the Grad-Shafranov equilibrium:

$$
\begin{aligned}
&rF_2' = \frac{\epsilon}{q^2}\left(\frac{\alpha}{2}-\epsilon(2-s)\right)\\
&\Delta' = \epsilon\left(\beta_p(r)+\frac{l_i(r)}{2}\right)\\
&r^2S_m''+[3-2s(r)]rS_m'+(1-m^2)S_m=0,
\end{aligned}
$$

where

$$
l_i(r) = 2\frac{q^2}{r^4}\int_0^r dr\,\frac{r^3}{q^2}\ ,\ \beta_p = \frac{q^2}{\epsilon r^3}\int_0^r dr\,r^2\frac{\alpha(r)}{q(r)^2}.
$$

The equation for F_2' has been used in the drift calculation in order to simplify algebra. The shaping terms are seen to be independent of pressure at this order. For vanishing local magnetic shear one obtains simply $S_m(r) \propto r^{m-1}$.

1. VMEC/ANIMEC coordinate transformation

An alternative to solving the differential equations above is to parameterise the analytical expansion coefficients employed in this paper in terms of widely used equilibrium codes. A straightforward example is conversion from the coordinates used in the VMEC/ANIMEC [23] codes in the axisymmetric limit and up-down symmetric limit. These codes use the Fourier representation:

$$
R = \sum_{l=0}^{\infty}\overline{R}_l(s)\cos lt \ \text{ and } \ Z = \sum_{l=0}^{\infty}\overline{Z}_l(s)\sin lt.
$$

One can then identify the required coefficients:

$$
\begin{aligned}
R_0 &= \overline{R}_0(s=0)\\
r &= \left(\overline{R}_1(s)+\overline{Z}_1(s)\right)/2\\
\Delta(r) &= \overline{R}_0(s=0)-\overline{R}_0(s)\\
S_2(r) &= \left(\overline{R}_1(s)-\overline{Z}_1(s)\right)/2\\
S_m(r) &= \overline{R}_{m-1}(s)\ \text{ for }\ m>2.
\end{aligned}
$$

The VMEC/ANIMEC codes can be used in such a way that the Fourier spectrum is minimised as much as possible. By restricting to $0 \le l \le 2$ the analytical results for the toroidal drift etc do not need to be extended to include squareness and higher order shaping (which penetrates weakly into the plasma since $S_m(r) \sim r^{m-1}$). Finally, the q profile and pressure profiles chosen for the VMEC/ANIMEC equilibrium then also give α and F_2.

2. CHEASE analytic shaped equilibria

The equilibrium coefficients used in this paper can be identified in terms of CHEASE [24] analytic equilibria:

$$
\begin{aligned}
R &= \hat{R}_0(\hat{r})+\hat{r}\cos(t+\delta(\hat{r})\sin t)\\
Z &= \hat{r}\kappa(\hat{r})\sin t.
\end{aligned}
$$

One then finds that

$$
\begin{aligned}
R_0 &= \hat{R}_0(\hat{r}=0)\\
r &= \frac{\hat{r}(\kappa(\hat{r})+1)}{2}\\
\frac{S_2(r)}{r} &= -\frac{\kappa(\hat{r})-1}{\kappa(\hat{r})+1}\\
\frac{S_3(r)}{r} &= \frac{\delta(\hat{r})}{4}\\
\Delta(r) &= \hat{R}_0(\hat{r}=0)-\hat{R}_0(\hat{r})+\frac{\hat{r}(\kappa(\hat{r})+1)\delta(\hat{r})}{8}.
\end{aligned}
$$

The q profile and pressure profiles chosen for the CHEASE equilibrium then also give α and F_2.

3. Soloviev equilibria

Flux surfaces of Soloviev equilibria are described by $R = \overline{R}_0(1+2\rho/\overline{R}_0\cos t)^{1/2}$ and $Z = \rho\kappa\sin(t)(1+2\rho/\overline{R}_0\cos t)^{-1/2}$. One then obtains approximately:

$$\begin{aligned} R_0 &= \hat{R}_0 \\ r &= \frac{\rho(\kappa+1)}{2}\left(1+\frac{1}{7}\frac{\rho}{R_0}\right) \\ \frac{S_2(r)}{r} &= -\frac{\kappa-1}{\kappa+1} \\ \frac{S_3(r)}{r^2} &= \frac{1}{R_0}\frac{\kappa}{(1+\kappa)^3} \\ \frac{\Delta(r)}{r^2} &= \frac{1}{R_0}\frac{2+3\kappa}{(1+\kappa)^3}. \end{aligned}$$

Moreover, as is well known, the q profile and pressure profile are constrained. The constants q_0 and κ entirely describe the equilibrium, and yield $F_2 = 0$. The resulting pressure gradient can be written in terms of α using the relation above between r and ρ giving finally:

$$\begin{aligned} q(\rho) &= q_0\frac{1}{2\pi}\int_{-\pi}^{\pi}\frac{dt}{(1+2(\rho/R_0)\cos t)^{3/2}} \\ \alpha(\rho) &= \frac{\rho}{R_0}\frac{q^2}{q_0^2}\frac{4(1+\kappa^2)}{(1+\kappa)(1+(2/7)\rho/R_0)} \end{aligned}$$

which can now be parameterised in terms of r.

[1] M. N. Rosenbluth and M. L. Sloan, Phys. Fluids **14**, 1725 (1971)
[2] J. W. Connor, R. J. Hastie and T. J. Martin, Nucl. Fusion **23**, 1702 (1983)
[3] M. Jucker, J. P. Graves, W. A. Cooper, G. A. Cooper, Phys. Plasmas **50**, 065009 (2008)
[4] Ya. I. Kolesnichenko, *et al* Phys. Plasmas **10**, 1449 (2003)
[5] F. Zonca *et al*, Nucl. Fusion **47**, 1588 (2007)
[6] K. L. Wong *et al*, Phys. Rev. Lett **85**, 996 (2000)
[7] A. Marinoni, *et al*, Plasma Phys. Control. Fusion, **51**, 055016 (2009)
[8] A. Merle, *et al*, Phys. Plasmas **19**, 072504 (2012)
[9] C. T. Hsu, *et al*, Phys. Fluids B **2**, 280 (1990)
[10] F. Porcelli *et al*, Phys. Plasmas **1**, 470 (1994)
[11] M. N. Bussac *et al* Phys. Rev. Lett **35**, 1638 (1975)
[12] B. B. Kadomstev, *Plasma Physics and the Problem of Controlled Thermo-nuclear Reactions* (Pergamon, London, 1960), Vol III, p285
[13] R. B. White and M. S. Chance, Phys. Fluids **27**, 2455 (1984)
[14] J. P. Graves, R. J. Hastie, K. I. Hopcraft, Plasma Phys. Control. Fusion **42**, 1049 (2000)
[15] E. Frieman and M. Rotenberg, Rev. Mod. Phys. **32**, 898 (1960)
[16] J. P. Graves, I. T. Chapman, S. Coda, M. Lennholm, M. Albergante and M. Jucker, Nature Commun. **3**, 624 (2012)
[17] J. P. Graves, I. T. Chapman, S. Coda, L. -G. Eriksson, T. Johnson, Phys. Rev. Lett. **102**, 065005 (2009)
[18] Hazeltine and Hinton, Rev. Mod. Phys. **48**, 239 (1976)
[19] P. Helander, R. J. Hastie, and J. W. Connor, Phys. Plasmas **4** (9), 3211 (1997)
[20] N. Madden and R. J. Hastie, Nucl. Fusion **34**, 519 (1994)
[21] Y. Wu C. Z. Cheng and R. B. White, Phys. Plasmas **1**, 3369 (1994)
[22] C. M. Roach, J. W. Connor and S. Janjua, Plasma Phys. Cont. Fusion **37**, 679 (1995)
[23] S. P. Hirshman and J. C. Whitson, Phys. Fluids **26**, 3553 (1983)
[24] H. Lutjens *et al*, Comp. Phys. Comm. **97**, 219 (1996)